A DIFFUSION BASED MODEL FOR THE INTERNAL CORROSION USING THE THERMOCHEMISTRY LIBRARY CHEMAPP[1]

Vicente Braz Trindade[2]
Ulrich Krupp[3]
Hans-Jürgen Christ[4]
Klaus Hack[5]

Abstract
The overall objective of this study is the simulation of high-temperature corrosion processes under near-service conditions, which requires both, a thermodynamic model to predict phase stabilities for given conditions and a mathematical description of the process kinetics, i.e., solid state diffusion. An outlook on the software package (***InCorr***) that is one of the final products of the European-project OptiCorr will be given. A computer program was developed in which the thermodynamic program library ChemApp is integrated into a numerical finite-difference diffusion calculation to treat internal oxidation, nitridation and carburization processes in various commercial alloys (Fe-, Cu- and Ni-base alloys). The model is capable to simulate multi-phase internal corrosion processes that are controlled by solid-state diffusion into the bulk metal as well as intergranular corrosion occurring in low-alloy steels by fast inward oxygen transport along the grain boundaries of the substrate.
Key words: Local thermodynamic equilibrium; High-temperature corrosion; Diffusion model; InCorr; Chemapp,

UM MODELO BASEADO EM DIFUSÃO PARA CÁLCULO DO PROCESSO DE CORROSÃO INTERNA USANDO A SUBROTINA TERMOQUÍMICA CHEMAPP

Resumo
O objetivo geral deste estudo é a simulação dos processos de corrosão em condições próximas às de serviço, as quais requerem tanto um modelo termodinâmico para prever as estabilidades das fases para dadas condições quanto uma descrição matemática da cinética de corrosão, exemplo, difusão no estado sólido. Uma visão geral do software ***InCorr*** que é um dos produtos finais do projeto da comissão européia – OptiCorr – é apresentada. Um programa de computador no qual a subrotina termoquímica ChemApp foi integrada em um modelo matemático usando o método numérico de diferenças finitas para simulação dos fenômenos de oxidação interna, nitretação e carbonetação em várias sistemas de ligas comerciais (Fe-, Cu-, e ligas de níquel). O modelo é capaz de simular processos de corrosão envolvendo várias fases que são controladas pela difusão no estado sólido no interior do grão da liga assim como pela difusão ao longo dos contornos de grão como o que acontece durante corrosão de aços baixa liga através do rápido transporte de oxigênio ao longo dos contornos de grão.
Palavras-chave: Equilíbrio termodinâmico local; Corrosão em altas temperaturas; Modelo de difusão; ChemApp; InCorr.

[1] *Technical Contribution to the 61st International Congress of the ABM, January 24-27th 2006, Rio de Janeiro – RJ – Brazil.*
[2] *Quality and R&D Manager, Dr.-Ing., Tubos Soldados Atlântico – TSA (Brazil) and Universität Siegen (Germany), vicente.trindade@tsa.ind.br, vicentebraz@yahoo.com.br*
[3] *Senior Engineer, Dr.-Ing. habil, Institut für Werkstofftechnik – Universität Siegen (Germany)*
[4] *Professor, Dr.-Ing. habil., Institut für Werkstofftechnik – Universität Siegen (Germany)*
[5] *Director Manager, Dr.rer. nat., GTT-Technologies – Aachen (Germany)*

1 INTRODUCTION

For alloys used in high temperature corrosive atmospheres, the capacity for the formation of a protective scale with high density, high stability, good adhesion and low growth rate, on the surface of the component is very important. Generally, Al_2O_3, SiO_2 and Cr_2O_3 are expected to protect materials against the serious high temperature degradation. While, for most materials the formation of a continuous protective scale is difficult due to the limitation from the content of protective oxides forming elements. If no protective scales are formed on the surface, or if cracks or other types of defects for rapid gaseous transport exist in the scale, internal corrosion can be possible, which decreases the lifetime for the component greatly. Recently developed computer simulation provides a very useful tool for the components lifetime prediction.

The developed computer program, called InCorr, at the university of Siegen in cooperation with the EU-project OPTICORR was designed to simulate different kind of corrosion on the gas/alloy system at high-temperatures. Internal corrosion, which is not possible to be treated by the classical Carl Wagner theory, can be calculated using a rigorous numerical and thermodynamic model. As a basis for all process modelling activities in the OptiCorr project the thermodynamic programmer's library ChemApp has been used. ChemApp presents the engine of the Equilibrium module of FactSage in the form of a set of programmable interface routines between the user's own main program and the actual Gibbs energy minimisation code that is called in the background. [(1)] Thus, rigorous Gibbs energy thermodynamics can be employed in a multitude of calculational environments. ChemApp is a commercial product available for general use from GTT-Technologies.

2 INCORR: SOFTWARE FOR SIMULATION OF INTERNAL/INWARDS CORROSION PROCESSES AT HIGH-TEMPERATURE

For the simulation of internal/inwards corrosion processes at high-temperatures a special tool has been developed which makes use of explicit diffusional kinetics on the one hand and the concept of local equilibrium thermodynamics on the other. For this purpose a link has been established between the numerical environment of MATLAB and the thermochemical library ChemApp.

In the framework of the EU project OPTICORR the applicability of *InCorr* has been extended from pure internal corrosion phenomena, like internal oxidation, carburization and nitridation, to the formation of multi-phase superficial oxide scales, which are formed, e.g. during high-temperature exposure of boiler steels.[(2,3)]

2.1 Physical Modelling

2.1.1 Internal corrosion

A theoretical description of internal corrosion process can be obtained by applying Carl Wagner's classical theory of internal oxidation.[(4)] When the concentration of a solute B in an alloy AB is lower than a critical value required for transition to superficial scale formation of the nitride, oxide, or carbide, internal precipitation of corrosion products takes place. Assuming a parabolic rate law for the

penetration depth ξ and applying Fick´s second law to the diffusion fluxes of solute B and the corrosive species O to the reaction front, kinetics of internal corrosion can be expressed by means of a simple parabolic equation:

$$\xi^2 = \frac{D_O c_O^s}{\nu c_B^0} t \,, \qquad (1)$$

where ξ is the penetration depth of internal corrosion products, c_O^s the concentration of the corrosive species at the surface, and c_B^0 the initial concentration of the reacting alloying element B. It is assumed that the diffusion coefficient D_O of the corrosive species is substantially higher than the one of the reacting alloying element D_B.

For simple systems, Wagner's theory can be applied to predict the penetration depth of internal corrosion as well as the concentration profiles of the solute B and the corrosive species O according to the equations 2 and 3 which can be derived from Ficks`s second law:

$$c_O(x,t) = c_O^s \left[\frac{\operatorname{erfc} \frac{x}{2\sqrt{D_O t}}}{\operatorname{erf}\gamma} \right] \qquad (2)$$

$$c_B(x,t) = c_B^s \left[\frac{\operatorname{erf} \frac{x}{2\sqrt{D_B t}}}{\operatorname{erf}\gamma\sqrt{\Phi}} \right] \qquad (3)$$

where Φ is the ratio between the diffusion coefficients of the corrosive species and the solute metal B ($\Phi = D_O/D_B$). The constant γ is given by equation 4:

$$\gamma = \sqrt{\frac{c_O^s}{2\nu c_B^0}} \,. \qquad (4)$$

A treatment of internal-corrosion problems that involve more than one precipitating species, compounds of moderate stability, high diffusivities of the metallic elements or time-dependent changes in the test conditions, e.g., temperature or interface concentrations, is not possible by applying equations 1 to 3. To simulate such systems the application of a numerical method to the diffusion differential equations and the thermodynamics of the system is required.

2.1.2 Oxidation of steels

The distribution and structure of grain boundaries play an important role for the kinetics of many high-temperature degradation processes since the transport of matter along interfaces is by orders of magnitude faster than throughout the bulk. Therefore, reducing the grain size, i.e., increasing the fraction of fast diffusion paths, may have a detrimental effect, as it is known for the creep behaviour of metals and alloys.[5] On the other hand, the high-temperature oxidation resistance of CrNi 18 8-type stainless steels, which are widely used for superheater tubes in power plants, can benefit from smaller grain sizes. As reported by Teranishi et al.[6] and Trindade et al.,[7] the formation of protective, Cr-rich oxides scales ($FeCr_2O_4$ and/or Cr_2O_3) is promoted by the fast outward flux of Cr along the substrate grain boundaries. A similar effect can be used by providing nanocrystalline surface layers on Ni-based superalloys. Wang and Young[8] have shown that an increase in the fraction of grain boundaries can decrease the critical Al concentration required for the establishment of a superficial Al_2O_3 scale on a material that usually forms a Cr_2O_3 scale.

It has been shown[7] that in the case of low-Cr steels, typically used for cooling applications in power generation up to temperatures of approximately 550°C, the beneficial effect of grain refinement disappears. Here, the grain boundaries seem to act as fast-diffusion paths for the oxygen transport into the substrate. As shown in Figure 1 the parabolic rate growth obviously decreases as the alloy grain size increases. Furthermore, the oxidation kinetics decreases as the Cr content increases for alloys with similar grain size.

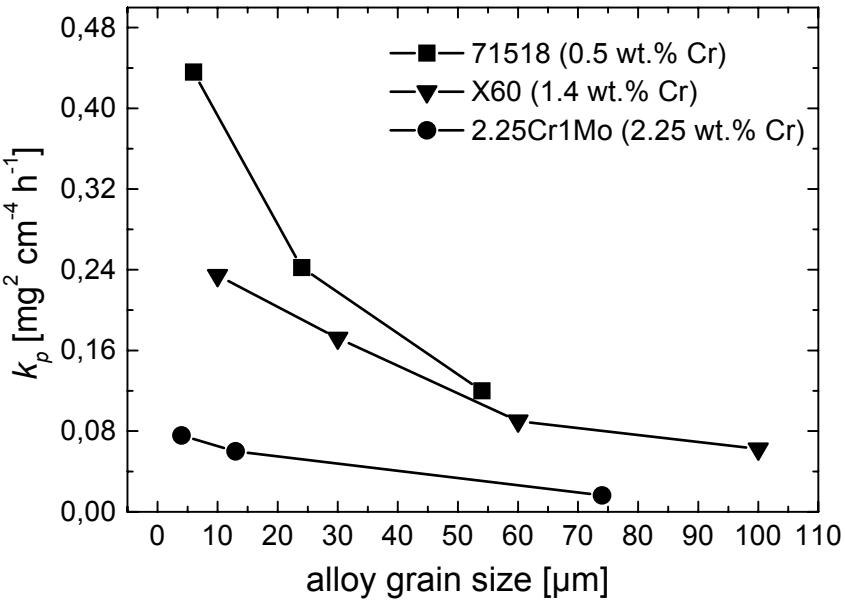

Figure 1. Parabolic rate constant k_p of three low-alloy steels oxidized in laboratory air at 550°C for 72 h.[3,7]

From inert-gold-marker experiments at 550°C (see Figure 2a) one knows that oxide scale growth occurs by both, outward Fe diffusion leading to the formation of hematite (Fe_2O_3, outermost) and magnetite (Fe_3O_4) and inward O transport leading to $(Fe,Cr)_3O_4$ formation. As a consequence of the Cr content in the substrate, a gradient in the Cr concentrations establishes reaching from the outer/inner scale interface (c_{Cr}=0) to the inner-scale/substrate interface, where the Cr concentration corresponds to the sole formation of the spinel phase $FeCr_2O_4$. This is in agreement with the thermodynamic prediction using a specific data set developed for these kinds of alloys.[9,10] The inward oxide growth itself is governed by an intergranular oxidation mechanism (Figure 2b) that can be described as follows: oxygen atoms that have reached the scale/substrate interface by short-circuit diffusion through cracks, pores[11,12] or by O anion transport penetrate into the substrate along the grain boundaries leading to the formation of Cr_2O_3 and, consequently, $FeCr_2O_4$. Progress of the scale/substrate interface occurs as soon as the bulk of the grains are oxidized completely.

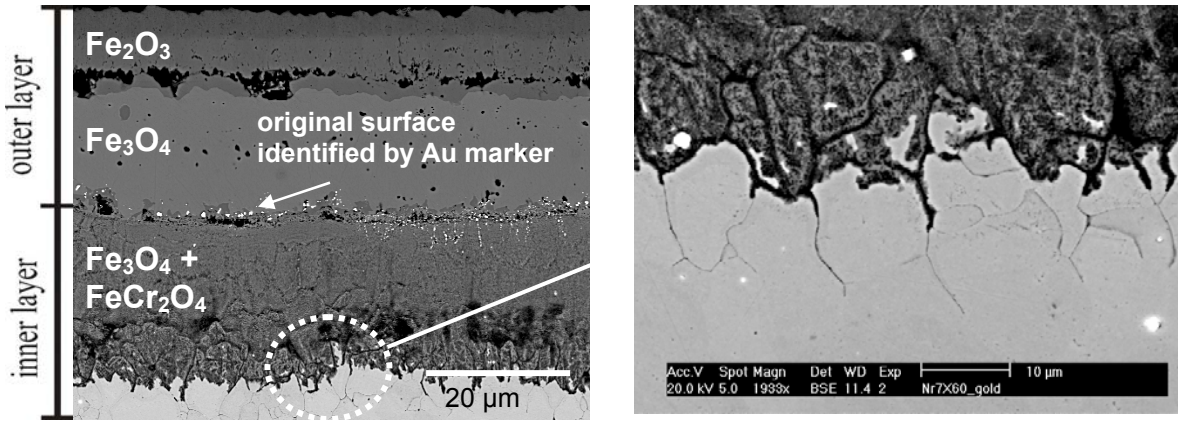

(a) (b)

Figure 2. (a) Oxide scale on a low alloy steel (grade X60) after expoosure at 550°C to laboratory air for 72h and (b) detail, showing the grain boundary attack underneath the interface inner scale/metal.(7)

2.1.3 Mathematical modelling and programming

Recently, a numerical model for the diffusive transport processes based on the finite-difference approach has been developed, which distinguishes between fast grain-boundary diffusion and bulk diffusion. Qualitatively, it is capable to predict the relationship between substrate grain size and inward oxide growth kinetics or internal precipitation. Together with the powerful thermodynamic tool ChemApp in combination with a data set for the Fe-Cr-O system the mechanism-based simulation of the overall oxidation process of low-Cr steels became possible. In this section, the mathematical background of the model will be described with emphasis on the inward oxide scale formation on low-Cr steels.

Generally, the generic driving force of high temperature corrosion processes can be separated into (i) transport mechanisms, i.e., solid-state diffusion in most cases, and (ii) thermodynamics of chemical reactions. The commonly used, phenomenological way to treat diffusion processes is the application of a second-order partial differential equation (Fick's 2nd law) formulating a relationship between the derivative of the concentration of a species *c* after the time *t* and its gradient by means of the location- and temperature-dependent diffusion coefficient *D*, which represents the jump frequency of the species within a substrate.

$$\frac{\partial c}{\partial t} = D\frac{\partial^2 c}{\partial x^2} \tag{5}$$

This equation can be rewritten in a simplified form for two-dimensional diffusion problems by neglecting any cross terms in the following form:

$$\frac{\partial c}{\partial t} = D_x \frac{\partial^2 c}{\partial x^2} + D_y \frac{\partial^2 c}{\partial y^2}, \tag{6}$$

where D_x and D_y are the diffusion coefficients in *x* and *y* direction, respectively. Through differential quotients according to the Crank-Nicolson finite-difference scheme (13), here represented in a simplified one-dimensional form:

$$\frac{\partial c}{\partial t} \approx \frac{c(x,t+\Delta t) - c(x,t)}{\Delta t} \tag{7}$$

$$\frac{\partial^2 c}{\partial x^2} \approx \frac{D_x}{2}\left(\frac{c(x-\Delta x,t+\Delta t)-2c(x,t+\Delta t)+c(x+\Delta x,t+\Delta t)}{\Delta x^2} + \frac{c(x-\Delta x,t)-2c(x,t)+c(x+\Delta x,t)}{\Delta x^2}\right). \quad (8)$$

By substituting the second derivatives in equation (5) by the corresponding difference quotients of the concentrations at the locations x-Δx, x, and x+Δx, as well as at y-Δy, y, and y+Δy, respectively, at the times t and t+Δt, one obtains the implicit Crank-Nicolson scheme of the finite-difference approach for two-dimensional diffusion.

$$\begin{aligned}\frac{c(x,y,t+\Delta t)-c(x,y,t)}{\Delta t} = {} & \frac{D_x(x,y)}{2}\cdot\frac{c(x-\Delta x,y,t)-2c(x,y,t)+c(x+\Delta x,y,t)}{\Delta x_l(x,y)\cdot\Delta x_r(x,y)} \\ & + \frac{D_x(x,y)}{2}\cdot\frac{c(x-\Delta x,y,t+\Delta t)-2c(x,y,t+\Delta t)+c(x+\Delta x,y,t+\Delta t)}{\Delta x_l(x,y)\cdot\Delta x_r(x,y)} \\ & + \frac{D_y(x,y)}{2}\cdot\frac{c(x,y-\Delta y,t)-2c(x,y,t)+c(x,y+\Delta y,t)}{\Delta y_l(x,y)\cdot\Delta y_r(x,y)} \\ & + \frac{D_y(x,y)}{2}\cdot\frac{c(x,y-\Delta y,t+\Delta t)-2c(x,y,t+\Delta t)+c(x,y+\Delta y,t+\Delta t)}{\Delta y_l(x,y)\cdot\Delta y_r(x,y)}\end{aligned} \quad (9)$$

The concept of the finite-difference equation (9) with locations of variable step widths Δx_l and Δx_r at the left- and right-hand side of x and Δy_l and Δy_r at the left- and right-hand side of y.

If applied to an area of the size $n\cdot\Delta x\cdot m\cdot\Delta y$, equation (9) can be rewritten as a matrix equation, valid for the concentrations $c(x,y)$ at each location, which can be expressed as concentration vectors $\vec{c}(t)$ and $\vec{c}(t+\Delta t)$ for successive time steps t and t+Δt. Since the right-hand side of equation (9) consists of elements of the concentration vectors at different locations according to Figure 5, it can be expressed by using the complete concentration vectors $\vec{c}(t)$ and $\vec{c}(t+\Delta t)$ multiplied with the corresponding matrices $\mathbf{M_x}$ and $\mathbf{M_y}$. The product of the matrix $\mathbf{B_x}$ and $\mathbf{B_y}$ with the boundary concentration vectors $\vec{c}_b(t)$ and $\vec{c}_b(t+\Delta t)$ is required to establish the boundary conditions in equation (9), e.g., at locations ahead of the boundary x_1 no valid concentration value for x_1-Δx within the finite-difference mesh does exist, therefore, it has to be defined by $c_b(x_1\text{-}\Delta x,y,t)$. Finally, the location-dependent diffusion coefficients $D(x,y)$ and the flexible step widths Δx_l and Δx_r, and Δy_l and Δy_r are expressed by the matrices $\mathbf{R_x}$ and $\mathbf{R_y}$, respectively:

$$\mathbf{R}_\mathbf{x} = \mathrm{diag}\left[\frac{D_x(x,y)}{2\Delta x_l\Delta x_r}\right] \text{ and } \mathbf{R}_\mathbf{y} = \mathrm{diag}\left[\frac{D_y(x,y)}{2\Delta y_l\Delta y_r}\right]. \quad (10)$$

Then, the matrix equation representing equation (9) for each location step of the finite-difference mesh can be written as follows:

$$\begin{aligned}\frac{1}{\Delta t}\left[\vec{c}(t+\Delta t)-\vec{c}(t)\right] = {} & \mathbf{R}_\mathbf{x}\left[\mathbf{M}_\mathbf{x}\vec{c}(t)+\mathbf{B}_\mathbf{x}\vec{c}_b(t)\right]+\mathbf{R}_\mathbf{x}\left[\mathbf{M}_\mathbf{x}\vec{c}(t+\Delta t)+\mathbf{B}_\mathbf{x}\vec{c}_b(t+\Delta t)\right] \\ & +\mathbf{R}_\mathbf{y}\left[\mathbf{M}_\mathbf{y}\vec{c}(t)+\mathbf{B}_\mathbf{y}\vec{c}_b(t)\right]+\mathbf{R}_\mathbf{y}\left[\mathbf{M}_\mathbf{y}\vec{c}(t+\Delta t)+\mathbf{B}_\mathbf{y}\vec{c}_b(t+\Delta t)\right]\end{aligned}. \quad (11)$$

When the boundary concentrations are assumed as (i) to be homogeneous and (ii) to experience only small changes, i.e., $\vec{c}_b(t)\approx\vec{c}_b(t+\Delta t)$, and the matrices in equation (11) are multiplied according to $\mathbf{M}=\mathbf{R_xM_x}+\mathbf{R_yM_y}$ and $\mathbf{B}=2(\mathbf{R_xB_x}+\mathbf{R_yB_y})$ one obtains the following governing equation for the concentration vector $\vec{c}(t+\Delta t)$ as a function of the concentration vector at the preceding time step $\vec{c}_b(t)$ and $\vec{c}(t)$:

$$\left[\frac{1}{\Delta t}\mathbf{E}-\mathbf{M}\right]\vec{c}(t+\Delta t)=\left[\frac{1}{\Delta t}\mathbf{E}-\mathbf{M}\right]\vec{c}(t)+\mathbf{B}\vec{c}_b(t), \qquad (12)$$

with the unit matrix **E**.

Implemented in the commercial simulation design environment MATLAB, equation (12) is solved for all species participating in the corrosion reaction and stepwise for the complete reaction time $p\cdot\Delta t$ according to the schematic representation in Figure 3 (simplified for one-dimensional diffusion).[3]

To accommodate for the possible chemical reactions of the ongoing corrosion process, the calculated concentrations at $\vec{c}(t+\Delta t)$ (c_i^{j+1} in Figure 3) must be corrected according to the local thermodynamic equilibrium. For this purpose, the concentrations $\vec{c}(t+\Delta t)$ are transferred into a thermodynamic subroutine ThermoScript, which contains the commercial program ChemApp. ChemApp is based on a numerical Gibbs' energy minimization routine in combination with tailor-made data bases. In order to avoid excessive calculation times, the parallel-computing system PVM (parallel virtual machine) is used, i.e., ThermoScript distributes the individual equilibrium calculations to thermodynamic workers according to the schematic representation in Figure 3. Therefore, by using, e.g., 200 parallel-working processing units (CPUs) the calculation time can be reduced by a factor of up to 200 as compared to a conventional PC. The complete sets of concentrations of all the participating species in local equilibrium form the new starting concentration vector $\vec{c}(t)$ for the application of equation (9) at the following time step *k*+2.

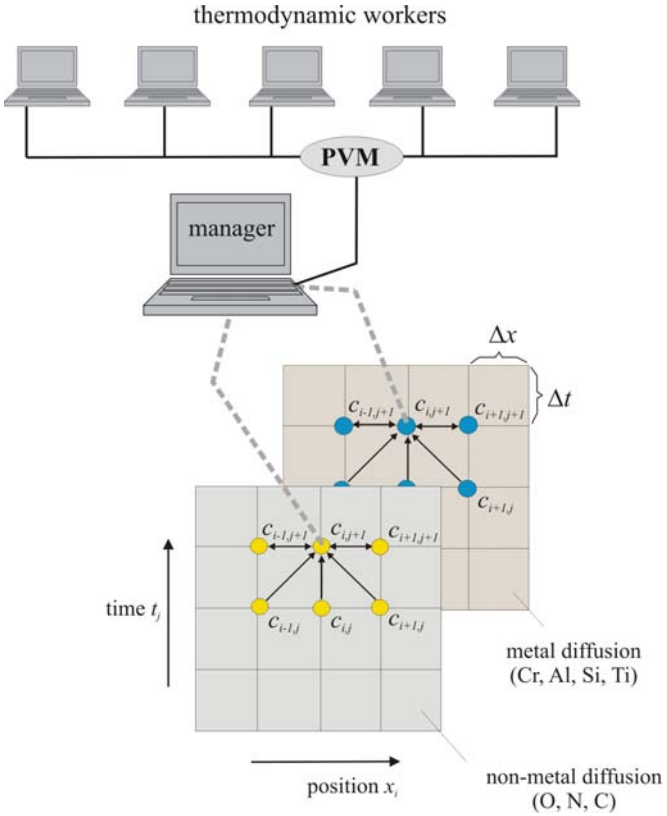

Figure 3. Schematic representation of the implicit finite-difference technique in combination with the thermodynamic program ChemApp.

3 SIMULATION OF INTERNAL/INWARD OXIDATION/CORROSION OF STEELS

To apply the finite-difference approach mentioned above to oxidation processes of Cr-containing steels, it has to be taken into account that, generally, the oxide scale consists of three or more separate layers, e.g., in the case of low-Cr steels an outer magnetite scale (below an outermost hematite layer) on top of an inward-growing magnetite/spinel-phase scale and an intergranular oxidation zone below the scale/substrate interface.

Since it was shown in the present project that oxidation processes of Cr-containing steels are mainly governed by grain-boundary transport of the reacting species, i.e, Cr and O grain-boundary diffusion, a two-dimensional finite-difference model has been established that distinguishes between fast diffusion along substrate grain boundaries and slow transport through the bulk. Due to the lack of data available for interface diffusivities, on the base of an estimate value for the grain boundary width[14] of δ=0.5nm, the grain-boundary diffusion coefficient was assumed to be 100 times higher than the bulk diffusion coefficient,[15] which has a value of D_b=5.39 10^{-13}m²/s for oxygen in iron at T=550°C.

According to the schematic representation for the intergranular oxidation process in low-Cr steels in Figure 4, oxygen firstly penetrates along the substrate grain boundaries, and hence, the diffusivity elements D_y of the matrix $\mathbf{R_y}$ along the grain boundaries are set to the grain boundary diffusion coefficient D_{GB}. At the same time oxygen bulk diffusion takes place driven by the two-dimensional concentration gradient. Hence, the respective elements D_x and D_y of the matrices $\mathbf{R_x}$ and $\mathbf{R_y}$ are set to the bulk diffusion coefficient D_b. The first oxidation product that becomes thermodynamically stable during this process is Cr_2O_3. The corresponding depletion in Cr in combination with the increase of the oxygen activity leads to the subsequent formation of the Fe-Cr spinel $FeCr_2O_4$. Further Cr depletion manifests itself in a Cr gradient in the $(Fe,Cr)_3O_4$ phase over the inward-growing oxide scale, finally resulting in almost pure magnetite (Fe_3O_4). As soon as the metallic substrate is completely consumed (except the residual Fe in equilibrium with Fe_3O_4) the inner-oxide/substrate interface moves one location step inward (see Figure 4).

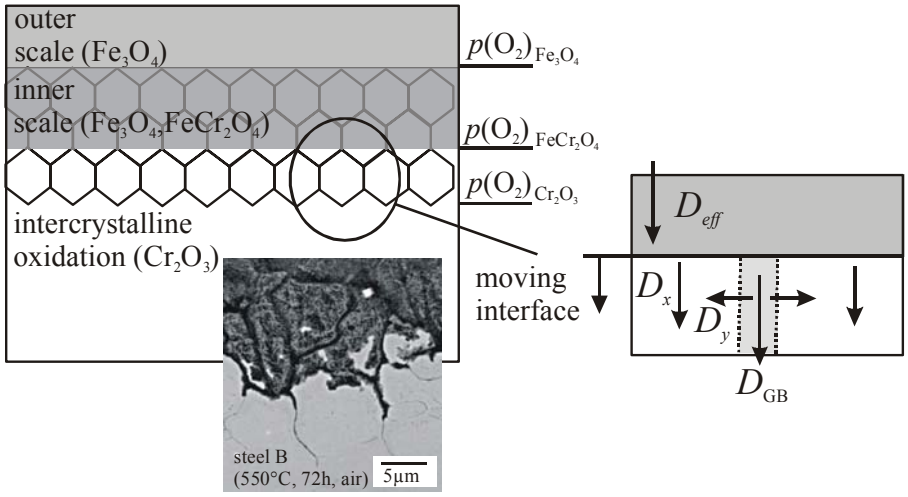

Figure 4. Schematic representation of the oxidation process of low-alloy Cr-containing steels and the two-dimensional model using a moving-interface approach and distinguishing between grain-boundary and bulk diffusion. [3,16]

Diffusion through the inner $Fe_3O_4/FeCr_2O_4$ scale, the mechanism of which is not fully understood since it strongly depends on the Cr concentration and is affected by the pronounced porosity, is treated in this study by an effective diffusion coefficient D_{eff}. The observed value of D_{eff} was estimated by means of the experimentally determined k_p value for the inner-scale growth kinetics in combination with Wagner's theory of oxidation.[17]

$$k_p = \int_{p(O_2)Cr_2O_3}^{p(O_2)Fe_3O_4} D_O \, d \ln p(O_2), \qquad (13)$$

where $p(O_2)Fe_3O_4$ is the oxygen partial pressure at the outer/inner scale interface (see 4) and $p(O_2)Cr_2O_3$ the estimated, respective pressure at the scale/substrate interface.

To distinguish the lattice diffusion (volume diffusion) from the diffusion along grain boundaries the diffusion coefficient matrix has to be set up before starting of the calculations. In this case the definition of the real diffusion coefficient matrix is:

$$D_{ij} = \begin{cases} D_b & \text{; if } (i,j) \text{ is located inside the grain} \\ D_{GB} & \text{; if } (i,j) \text{ is located along grain boundaries} \end{cases}$$

However, when the parent element, e.g. iron, oxidizes, than it is necessary to distinguish also between the diffusion in the oxide and diffusion in the substrate bulk and along grain boundaries. This has been realized by implementation of a moving interface which is used the calculation of inward scale formation in steels.

For this more complex case the diffusion matrix becomes:

$$D_{ij} = \begin{cases} D_b & \text{; if } (i,j) \text{ is located inside the grain and } c_{Fe}>0 \\ D_{GB} & \text{; if } (i,j) \text{ is located along grain boundaries and } c_{Fe}>0 \\ D_{oxide} & \text{; if } (i,j) \text{ is located in the region where } c_{Fe}=0 \end{cases}$$

The numerical model described was applied to the oxidation processes of low- and high-Cr steels using diffusion data given by Heuman.[15]

- $D_{O \text{ in } \alpha\text{-Fe}}=2.8\text{x}10^{-4}$ exp (-251kJ/RT),
- $D_{Cr \text{ in } \alpha\text{-Fe}}=3.59\text{x}10^{-6}$ exp (-179kJ/RT),
- $D_{Fe \text{ in } \alpha\text{-Fe}}=3.78\text{x}10^{-7}$ exp (-92.1kJ/RT).

Figure 5 shows the calculated two-dimensional concentration profiles for magnetite (Fe_3O_4), the Fe-Cr spinel phase ($FeCr_2O_4$) and chromia (Cr_2O_3) for steel X60 containing 1.44wt.% Cr and having a grain size of d=30µm. It should be mentioned here that the thermochemical database of the system treats Fe_3O_4 and $FeCr_2O_4$ as separate but coexisting phases, i.e., an increase in the Cr concentration leads to a relative increase in the fraction of the spinel phase $FeCr_2O_4$.

The results support the experimental observation that the first oxide phase being formed is Cr_2O_3 along the substrate grain boundaries, followed by $FeCr_2O_4$ and finally, Fe_3O_4. Since oxygen penetration into the alloy occurs by both, grain-boundary as well as bulk diffusion, the oxidation process proceeds from the grain boundaries into the bulk until the complete metallic phase is consumed. This situation defines the progress of the inner oxide scale (see arrow in Figure 5a).

The simulated growth kinetics of the inner oxide scale as a function of the exposure time is shown in Figure 6 for three different grain sizes. In the case of the material with a grain size of d=10µm it could be demonstrated that the simulated data are in excellent agreement with the experimentally determined values of the inner-scale thickness for various exposure times.

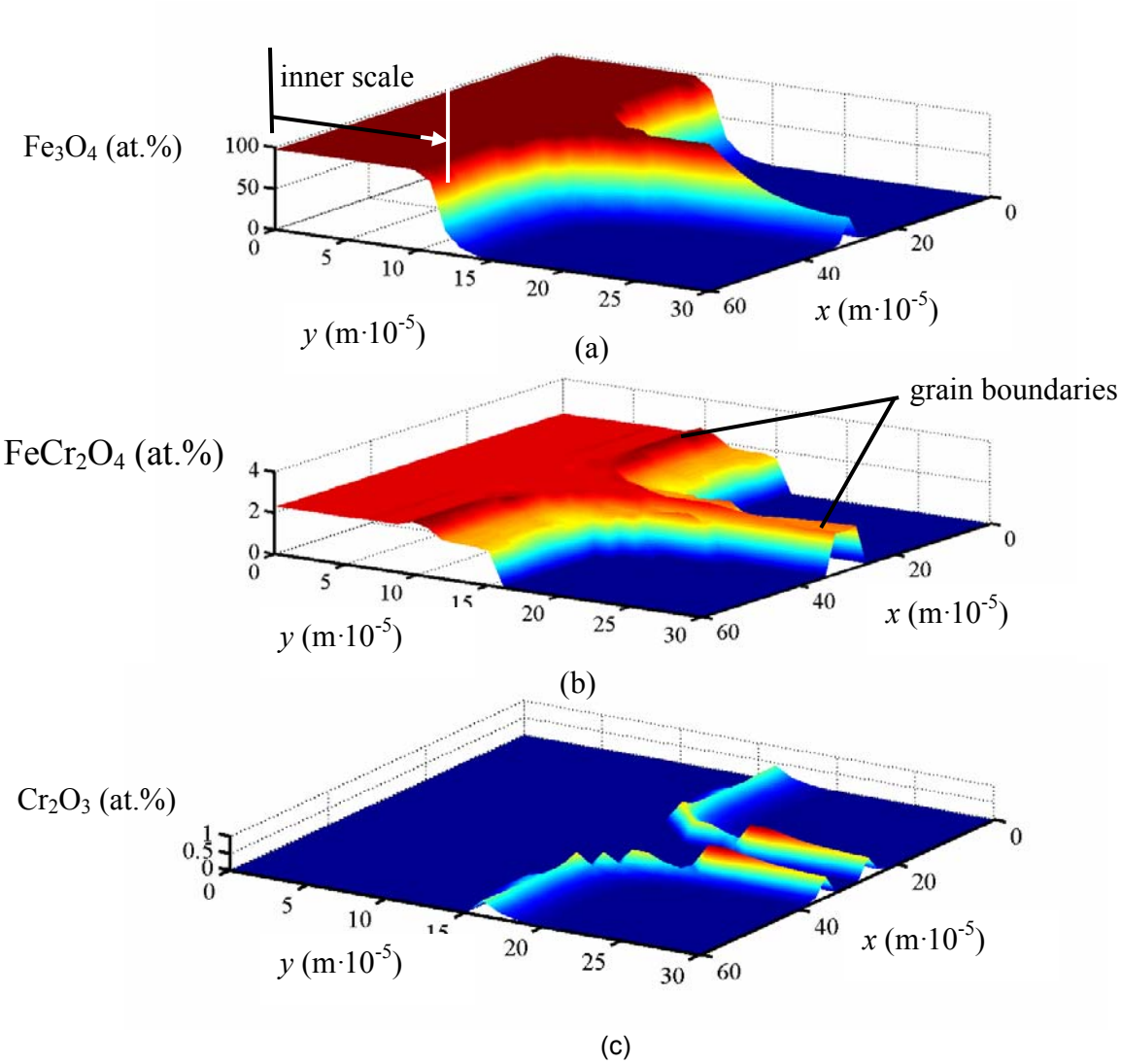

Figure 5. Simulated lateral concentration profiles of the oxide phases (a) Fe_3O_4, (b) $FeCr_2O_4$, and (c) Cr_2O_3 formed during exposure of the low-alloy steel X60 (c_{Cr}=1.44wt.%) with a grain size of d=30µm at T=550°C to air (y=0 corresponds to the original inner-scale/metal interface at t=0s).

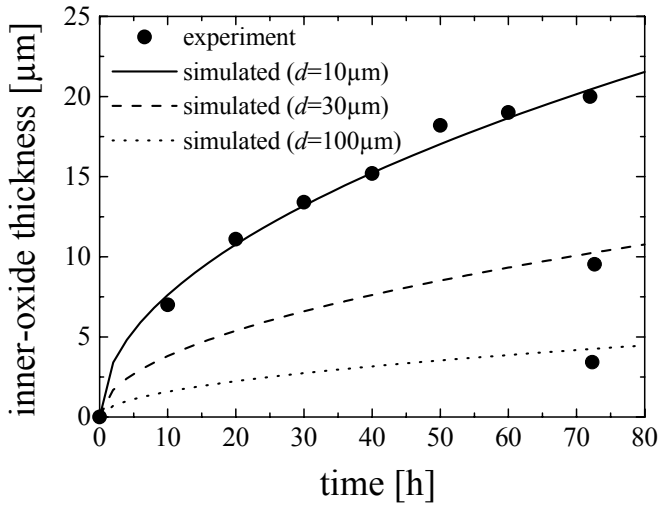

Figure 6. Comparison of the simulated inner-oxide growth kinetics for the low alloy steel X60 (c_{Cr}=1.44wt.%) with three different grain sizes and with the experimentally measured inner-oxide thickness for specimens having different grain sizes.

While for low-alloy steels with initial Cr concentrations between 0.5 and 2.3 wt.% an increase in the grain size results in a decrease in the oxidation kinetics, high-Cr austenitic steels exhibit a contrary effect: a smaller grain size results in an increase of the outward Cr transport and hence, to a transition in the oxidation mechanism from non-protective magnetite/spinel phase $(Fe,Cr)_3O_4$ to protective chromia (Cr_2O_3) formation. Experimental observations revealed that on top of the fine-grained specimens (d=4 and 11µm) a very thin protective Cr_2O_3 scale was formed. However, locally the oxide scale was not totally protective leading to the formation of iron oxide nodules, which grow outward and inward. Generally, the formation of a protective Cr_2O_3 scale on specimens with a small grain size is favoured by a higher Cr flux from the bulk to the substrate/oxide interface as a consequence of the higher grain boundary density. This is supported by first simulation results using the two-dimensional finite-difference approach as already described in combination with diffusion data taken from Kaur et al.[16] Figure 7 shows qualitatively the Cr enrichment and gradient along a substrate grain boundaary for high-temperature exposure of the austenitic stainless steel TP347. Indeed, the simulation revealed for an increase in the grain size, while keeping all the other parameters the same, that instead of pure Cr_2O_3 a mixture of oxide phases is formed as it is shown elsewhere.[3,17]

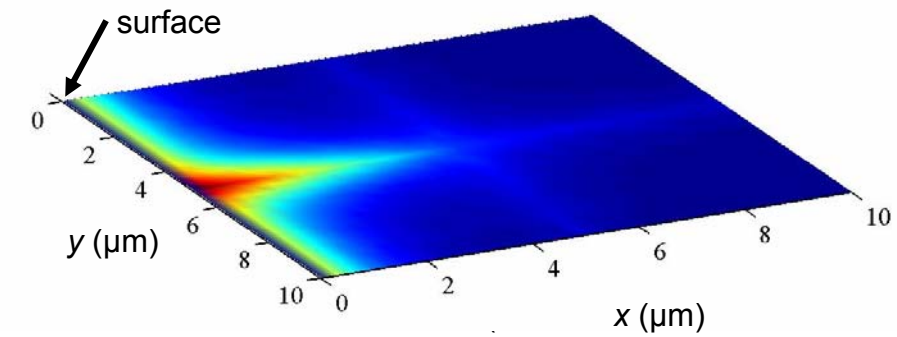

Figure 7. Qualitative Cr enrichment along substrate grain boundary on a fine-grained material (d=5µm) forming a superficial Cr_2O_3 scale.

4 CONCLUDING REMARKS

The examples presented above demonstrate the applicability of the combination of the finite-difference technique and computational thermodynamics to complex corrosion processes which depend substantially on the material's microstructure. Of course, much more experimental work is required to describe in detail the variety of possible transport processes, e.g., taking place within the porous inner oxides scale and along the substrate grain boundaries. Strictly spoken, the structure of the interfaces should change as soon as the grain boundaries are covered by an oxide phase which is in contact with the matrix on both sides. Also, the actual value of the grain-boundary thickness and its implementation in the finite difference approach remains an open question. In the present approach, the grain-boundary thickness is assumed as to be δ=0.5nm according to Fisher[3] and the segregation factor as to be s=1.

REFERENCES

1 G. Ericksson, K. Hack, Metallurgical Transactions B, 1990, 21B, 222.

2 V. B. Trindade, U. Krupp, H.-J. Christ, S. Yang, J. Gegner: *Proc. 3rd International Conference on Mathematic Modeling and Computer Simulation of Materials Technologies*, MMT3, 6.-10. September, Ariel, Israel (2004) 1.38-1.45.

3 V.B. Trindade, 2005, Hochtemperaturoxidation Cr-legierter Staelen: und von Ni-Basislegierungen: Experimentelle Untersuchung und Computersimulation (Oxidação em altas temperaturas de aços ligados com cromo e ligas de níquel: caracterização experimental e simulação computacional), Universitaet Siegen, Germany.

4 C. Wagner, *Zeitschrift für Physikalische Chemie*, 1933, *21*, 25

5 A. P. Sutton, R.W. Balluffi, *Interfaces in Crystalline Materials*, Oxford University Press, Oxford 1995.

6 H. Teranishi, Y. Sawaragi and M. Kubota, *The Sumitomo Research*, 1989, *38*, 63.

7 V.B. Trindade, U. Krupp, Ph. E.-G. Wagenhuber and H.-J. Christ, *Materials and Corrosion*, 2005, 56, 785.

8 F. Wang and D.J. Young, *Oxidation of Metals*, 1997, *48*, 497.

9 L. Heikinheimo, D. Baxter, M. Spiegel, K. Hack, U. Krupp, M. Hämäläinen, M. Arponen, *Proc. 6th International Symposium on High Temperature Corrosion and Protection of Materials*, Les Embiez, France, 461-464, 2004.

10 V. B. Trindade, U. Krupp, H.-J. Christ, 2005, Opticorr Guide Book, Capítulo 2 e 3, VTT Research Center, Finland.

11 R.Y. Chen and W.Y.D. Yuen, *Oxidation of Metals*, 2003, *59*, 433.

12 M. Schütze, online *Journal of Corrosion Science and Engineering*, 2003, *6.*

13 J. Crank, *The Mathematics of Diffusion*, 2nd edition, Clarendon Press, Oxford 1986.

14 J.C. Fisher, *Journal of Applied Physics*, 1951, *22*, 74.

15 T. Heumann, *Diffusion in Metallen*, Springer-Verlag, Berlin Heidelberg, Germany 1992.

16 I. Kaur, W. Gust, L. Kozma, *Handbook of Grain and Interphase Boundary Diffusion Data*, Ziegler Press, Stuttgart, Germany 1989.

17 U. Krupp, V. B. Trindade, H.-J. Christ, U. Buschmann, W. Wiechert, Diffusion and Defects Forum, 2004, 237-240, 946.